J Sol-Gel Sci Technol (2013) 68:479–487
DOI 10.1007/s10971-012-2946-9

ORIGINAL PAPER

Luminescent sol–gel materials based on lanthanide aminopolycarboxylates (Ln = Nd, Eu, Tb, Yb)

Evgen Fadeyev · Sergii Smola · Olga Snurnikova · Oleksandr Korovin · Natalya Rusakova

Received: 1 November 2012 / Accepted: 18 December 2012 / Published online: 3 January 2013

Abstract Luminescent organic–inorganic hybrid materials containing immobilized lanthanide(III) complexes (Ln = Nd, Eu, Tb, Yb) with modified ethylenediaminetetraacetic and diethylenetriaminepentaacetic acid were synthesized by sol–gel method. Obtained hybrids exhibit 4f-luminescence in the visible (Eu(III) and Tb(III)) and IR-region (Nd(III) and Yb(III)). The influence of the hybrid matrix on the lanthanide luminescence was established and it was shown, that the location of resonance level of Eu(III) is optimal for efficient energy transfer from matrix, while in the case of Tb(III) energy transfer does not occur and Tb(III) is able to absorb energy only due to its own week f–f transitions. It was also established that the inorganic matrix leads to elimination of nonradiative energy losses and increase of 4f-luminescence lifetimes. Covalent binding of Ln(III) aminopolycarboxylates in the matrix allows to consider obtained materials as promising for creation of photo- and chemically-stable luminescent sensors.

Keywords Sol–gel route · Organic–inorganic hybrids · Lanthanide(III) aminopolycaboxylates · 4f-luminescence

1 Introduction

In the past few decades luminescent compounds have been investigated as active components of nanomaterials and applied in different optical devises. In particular, lanthanide-containing compounds have a wide variety of photonic applications due to their narrow-line characteristic luminescence and large values of excited states lifetimes [1, 2]. The advantage of organic–inorganic hybrid materials is a successful combination of spectral-luminescent properties of lanthanide complexes and physicochemical properties of inorganic matrices. In such hybrids inorganic compounds, which form a rigid spatial lattice, are combined at a molecular level with the fragments of organic/metalorganic functional units evenly distributed into materials. The benefit of them compared with the materials based on polymeric matrices is simplicity and cheapness of their production, high optical quality and chemical purity. They are characterized by high chemical, thermal and photostability, an extensive pore system with controlled size [3, 4]. These materials in the form of ceramic powders, glasses, tapes and fibers are promising as potential components of LEDs, biomedical labels, lasers, fluorescent molecular thermometers, fluorescent sensors and optical amplifiers [3–8].

Sol–gel route is the optimal way for obtaining hybrid organic–inorganic materials based on lanthanide complexes. The main advantage of this method compared with the synthesis in the melt is lower temperatures of sol–gel process and, consequently, the lack of crystallization processes accompanied by phase separation.

Sol–gel method allows to obtain materials based on oxides of silicon, titanium, aluminum, zirconium, hafnium, germanium, etc. [3]. However, only in the case of silicon matrix there is a wide choice of precursors. In general, an increase of luminescent characteristics is observed for complexes included in siloxane matrix as a result of decrease in non-radiative energy losses due to rigidity and inertness of inorganic carrier [4, 5].

Organic–inorganic hybrid materials depending on the synthetic method are divided into two main types [3, 6]. In

E. Fadeyev · S. Smola · O. Snurnikova · O. Korovin · N. Rusakova (✉)
Department of Chemistry of Lanthanides A.V. Bogatsky Physico-Chemical Institute, National Academy of Sciences of Ukraine, Lustdorfskaya Doroga 86, 65080 Odessa, Ukraine
e-mail: natalirusa@yandex.ua; lanthachem@ukr.net

the first case, materials without covalent fixing of ligands/complexes in the matrix are formed only due to the relatively weak hydrogen bonds, ion–dipole and Van-der-Waals interactions. The second ones are covalently bonded hybrids that are prepared by stepwise synthesis. The first step is the modification of the ligand by functional group capable to form covalent bonds with products of hydrolysis of alkoxysilane during the polycondensation stage. Then the stage of complex formation takes place. At last, obtained complex is added to the sol–gel system during hydrolysis stage. The advantages of this method compared with the first one are stability of the resulting materials and uniform distribution of the emitting centers in an inorganic matrix.

Aminopolycarboxylic acids were chosen as precursor ligands for obtaining of luminescent lanthanide sol–gel materials in view of high stability of aminopolycarboxylates, allowing them to persist under the influence of both acidic and basic media of sol–gel process, and a wide possibility of chemical modification of ligands. This work presents synthesis and investigation of organic–inorganic hybrids containing covalently immobilized complexes of ethylenediaminetetraacetic and diethylenetriaminepentaacetic acids with lanthanide(III) ions that exhibit luminescence in the visible (Eu(III) and Tb(III)) and IR-region (Nd(III) and Yb(III)).

2 Experimental

2.1 Materials

Tetraethylorthosilicate (TEOS) (3-aminopropyl)trimethoxysilane (APTMS), ethylenediaminetetraacetic acid (EDTA), diethylenetriaminepentaacetic acid (DTPA) and their dianhydrides (EDTA-DA, DTPA-DA), concentrated hydrochloric and acetic acids, sodium hydroxide and organic solvents were purchased from Aldrich in reagent grade ≥98 % and used without further purification. Lanthanide acetates ($Ln(CH_3COO)_3{\cdot}xH_2O$) and aminopolycarboxylates (Ln-EDTA, Ln-DTPA, Ln = Nd, Eu, Tb, Yb, Lu) were prepared from the corresponding oxides (99.98–99.99 %, "Aldrich").

2.2 Synthesis of modified aminopolycarboxylic acids and lanthanide complexes

The syntheses were performed according to Scheme 1. Aminopolycarboxylic acid dianhydride (EDTA-DA or DTPA-DA, 5 mmol) was dissolved in 150 ml of anhydrous dimethylformamide (DMF) under stirring at 80 °C. Then an equimolar amount of (3-aminopropyl)trimethoxysilane (APTMS) was added dropwise. Synthesis was continued under stirring at 80 °C for 48 h. After that, 100 ml of tetrahydrofuran (THF) were added; precipitated white solid was filtered and recrystallized from a solvent mixture DMF-benzene (1:1).

For preparation of lanthanide complexes LnL1 and LnL2 (Ln = Nd(III), Eu(III), Tb(III), Yb(III), Lu(III)) modified ligand (L1 or L2, 0.50 mmol) was dissolved in 20 ml of distilled water by adding of 0.5 M sodium hydroxide solution until pH = 8 under heating. After that 0.55 mmol of $Ln(CH_3COO)_3{\cdot}xH_2O$ was added followed by reflux for 1 h. Then the solution was evaporated to dryness and the solid residue was recrystallized from EtOH. Complex with paramagnetic ion Lu(III) was obtained for NMR spectroscopic studies.

2.3 Synthesis of lanthanide doped luminescent hybrid materials

Tetraethylorthosilicate (TEOS, 5 mmol) was dissolved in 2.5 ml of EtOH and 1 ml of 0.1 mol/l HCl was added (pH = 1.5). The mixture was stirred for 30 min at 70 °C. Then a solution of lanthanide(III) complex (LnL1 or LnL2, 0.1 mmol) in 5 ml of water was added and reaction mixture was stirred for another 30 min at 70 °C. Then the solutions were placed into plastic container, covered with film and left to stand overnight at room temperature for gelation. The resulting samples were dried at 60 °C for 7 days, at 100 °C for 5 days and at 120 °C and reduced pressure (about 30 mmHg) for 20 h. Obtained transparent gels were grounded into the powder for further studying. The molar ratio of the components in the synthesis was TEOS:Complex:H_2O = 50:1:3,000. Pure silica-gel was also prepared as described above, without the addition of the complex.

2.4 Chemico-physical characterization

The resulting compounds and materials have been characterized by elemental analysis, ESI-mass spectrometry, FT-IR and ^{1}H NMR spectroscopy.

Elemental analysis (C, H, N) was carried out on Perkin-Elmer CHN-240 analyzer. The lanthanide content in the complexes was determined by complexometric titration.

ESI-Mass spectra were recorded on Waters ESI TOF Premier spectrometer. ^{1}H NMR spectra were obtained on Bruker Avance AV 400 (400 MHz) spectrometer in D_2O solutions at pH ≈ 10 (with the addition of NaOD) at 25 °C. IR spectra were recorded on Perkin-Elmer Frontier FT-IR spectrometer in KBr pellets.

Excitation, molecular fluorescence and 4f-luminescence spectra of solid samples were recorded on a Fluorolog FL 3-22 spectrofluorometer (Horiba Jobin-Yvon, Xe-lamp 450 W) at 25 °C. Microphotography was performed on Mira 3 Tescan scanning electron microscope.

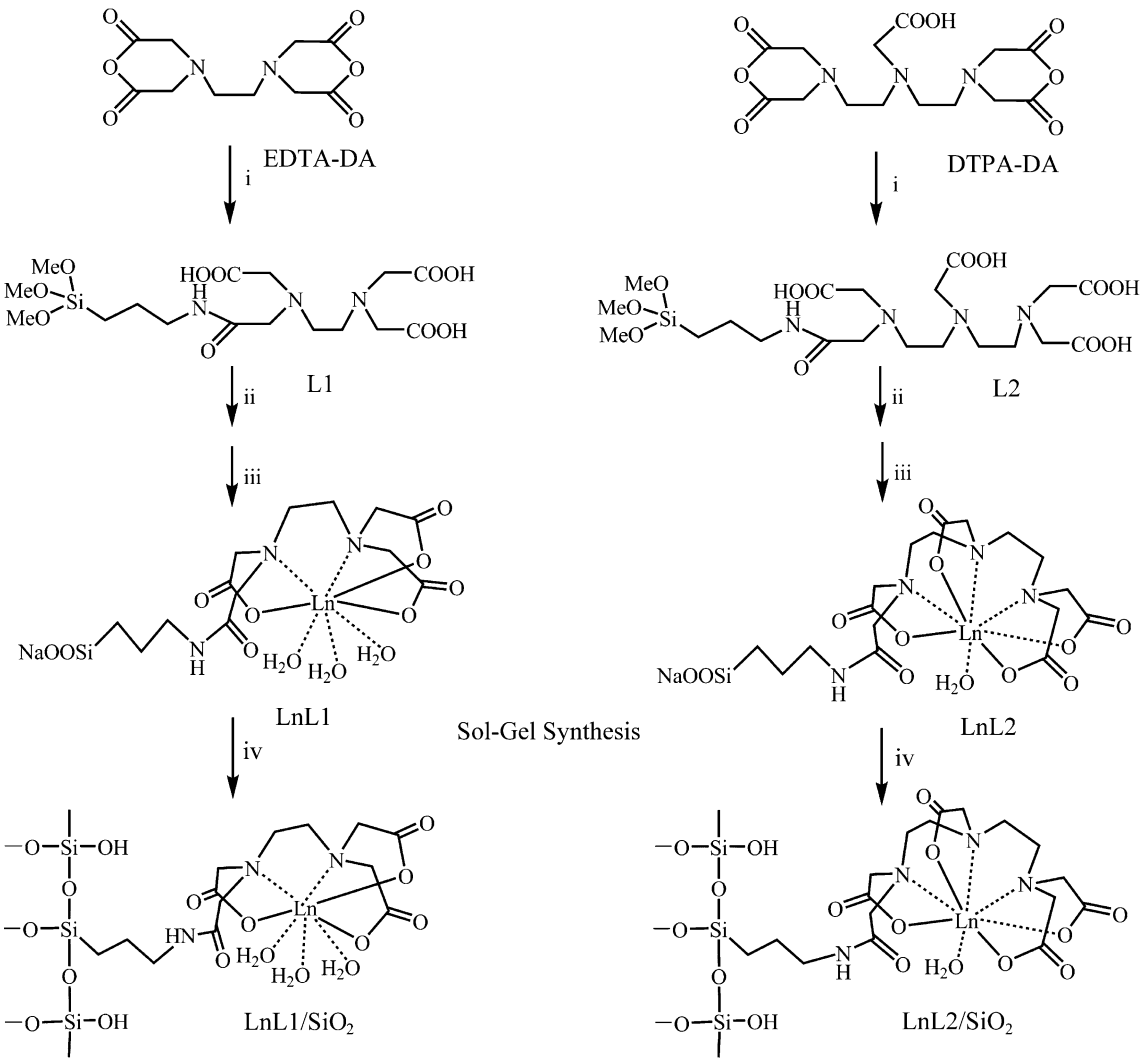

Scheme 1 Synthesis of silica-gels, containing lanthanide complexes with modified EDTA and DTPA. Reagents and conditions: (*i*) APTMS, DMF, 80 °C, 48 h; (*ii*) 0.5 M NaOH (pH = 8), H_2O; (*iii*) $Ln(CH_3COO)_3$, H_2O, 100 °C, 1 h; (*iv*) TEOS, H_2O, EtOH, HCl (pH = 2–3), 70 °C, 30 min

3 Results and discussion

Modified aminopolycarboxylic acids (L1, L2) are white solids that are soluble in water at pH > 7 and slightly soluble in DMF and DMSO. It is known that in aqueous solution hydrolysis of trimethoxysilyl groups takes place resulting in the formation of silanol groups Si–OH, capable of condensation with forming of siloxane bonds Si–O–Si [9]. When sodium hydroxide is added to solution (pH > 8) sodium salts with general formula $RSiOONa{\cdot}xH_2O$ are formed. They can exist in the form of isolated molecules as well as oligomers $(RSiOONa)_n{\cdot}xH_2O$, and these forms can coexist simultaneously in solution and in solid state.

Mass spectrometry and ^1H NMR spectroscopy data confirm the attachment of trimethoxysilylpropyl substituent to the EDTA and DTPA molecule. Only "soft" ionization methods such as MALDI or ESI are suitable for registration of the mass spectra of aminopolycarboxylic acids derivatives. ESI-mass spectra of ligands and complexes were recorded for freshly prepared water solutions, where both hydrolyzed and non-hydrolyzed forms of compounds were detected. In mass spectra of L1, L2 and their complexes besides the molecular ion peak other peaks corresponding to fragments with breaking bonds in trimethoxysilylpropyl substituent or glycine groups could be observed. In the mass spectra of the complexes there are also few peaks corresponding to the stepwise separation of coordinated water molecules from the molecular ion.

The ^1H NMR spectra of ligands and Lu(III) complexes were compared in order to investigate the coordination mode of the Ln(III) ion. In NMR-spectra of L2 (Fig. 1a), for instance, two triplets at 2.97–3.9 ppm from signals of ethylenediamine fragments, two singlets at 3.33–3.49 ppm from glycine fragments and three signals corresponding to

three methylene groups of propyl fragment at 0.59, 1.67–2.90 ppm are observed.

The complexation with Lu(III) ions leads to the shift of propyl fragment proton signals to low field region on 0.10–0.12 ppm (Fig. 1b). Instead of two triplets of ethylenediamine groups and two singlets from glycine protons, four triplets at 2.55–2.97 ppm and multiplet at 3.25–3.50 ppm appear in the spectrum of complex. Similar changes in the spectra are typical for lanthanide aminopolycarboxylates, since the coordination of the metal limits the conformational rotation around single C–C and C–N bonds, which leads to the magnetic nonequivalence of protons that are equivalent in the case of initial ligands [10, 11].

The interpretation of FT-IR spectroscopy data was carried out according to the literature for similar samples [12]. Fig. 2 shows the FT-IR spectra of the samples L2, EuL2 and EuL2/SiO_2. In the spectrum of L2 (Fig. 2a) compared with DTPA the band at 911 cm^{-1} and the broad band at 1,052–1,144 cm^{-1} corresponding to the asymmetric and symmetric stretching vibrations of Si–O–C bonds appear. The signal at 480 cm^{-1} corresponds to the bending vibrations O–Si–O. The peak at 694 cm^{-1} is probably caused by the stretching vibrations Si–C. The bands at 1,634 and 1,398 cm^{-1} are attributed to ν_{as} (COO^-) and ν_s (COO^-) and they do not change their position compared with DTPA. The shoulder at 1,733 cm^{-1} corresponds to unionized carboxyl groups. The band of bending vibrations of aminogroup, which presents in the spectrum of APTMS at 1,577 cm^{-1}, does not appear in the spectrum of L2 that confirms formation of amide bond, which band probably overlaps with the wide band of the ionized carboxyl groups. The peaks of C–H stretching vibrations are located at 2,936, 2,972 and 3,026 cm^{-1}.

In the FT-IR spectrum of the complex EuL2 (Fig. 2b) the band ν_{as} (COO^-) is shifted to 1,594 cm^{-1}, that is caused by the coordination of these groups with europium ion. The broad band at 2,546–2,550 cm^{-1} in the spectra of DTPA and L2, probably corresponding to stretching vibrations R_3N^+–H, disappears in the spectrum of complex. The

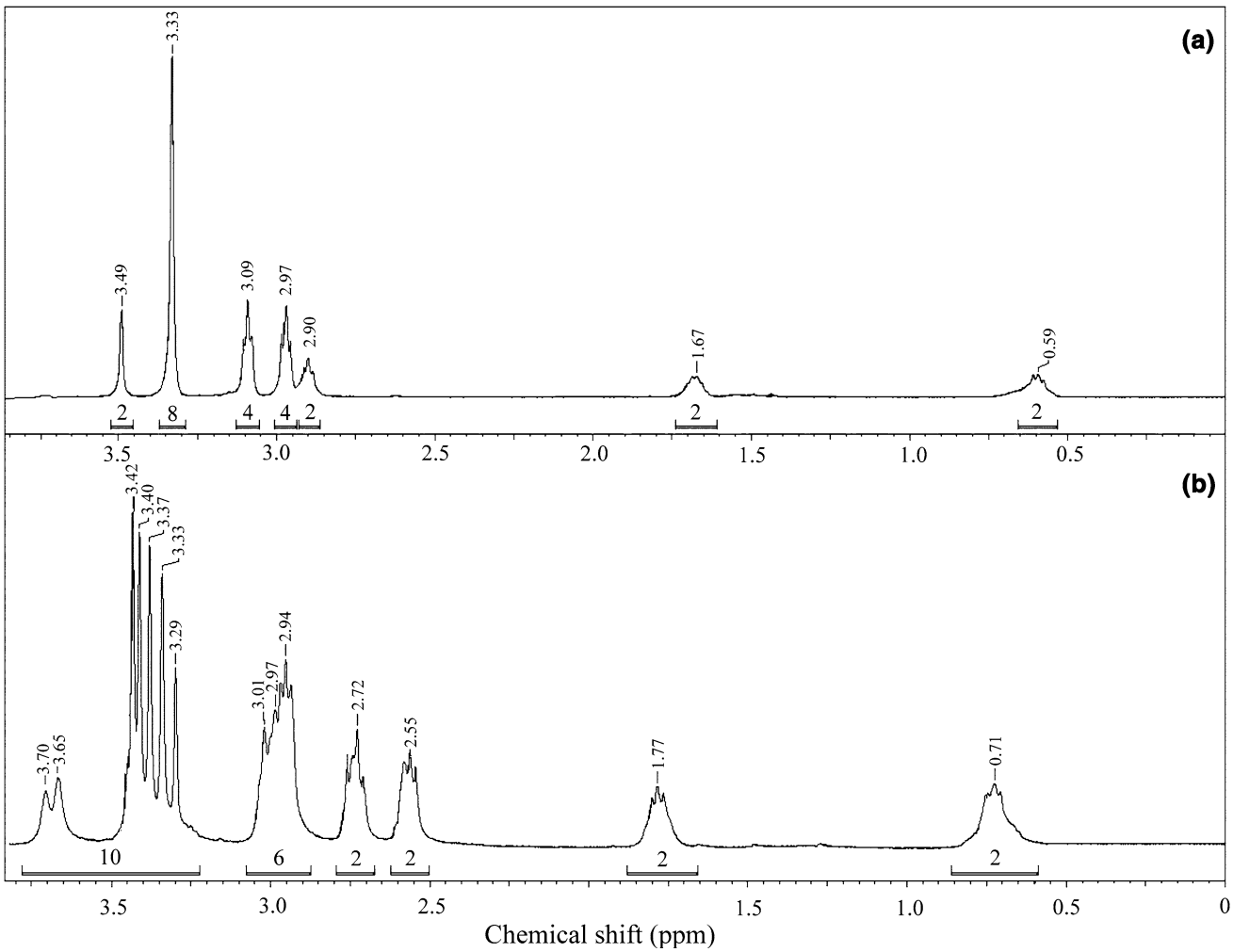

Fig. 1 ^{1}H NMR spectra of L2 (*a*), and LuL2 (*b*)

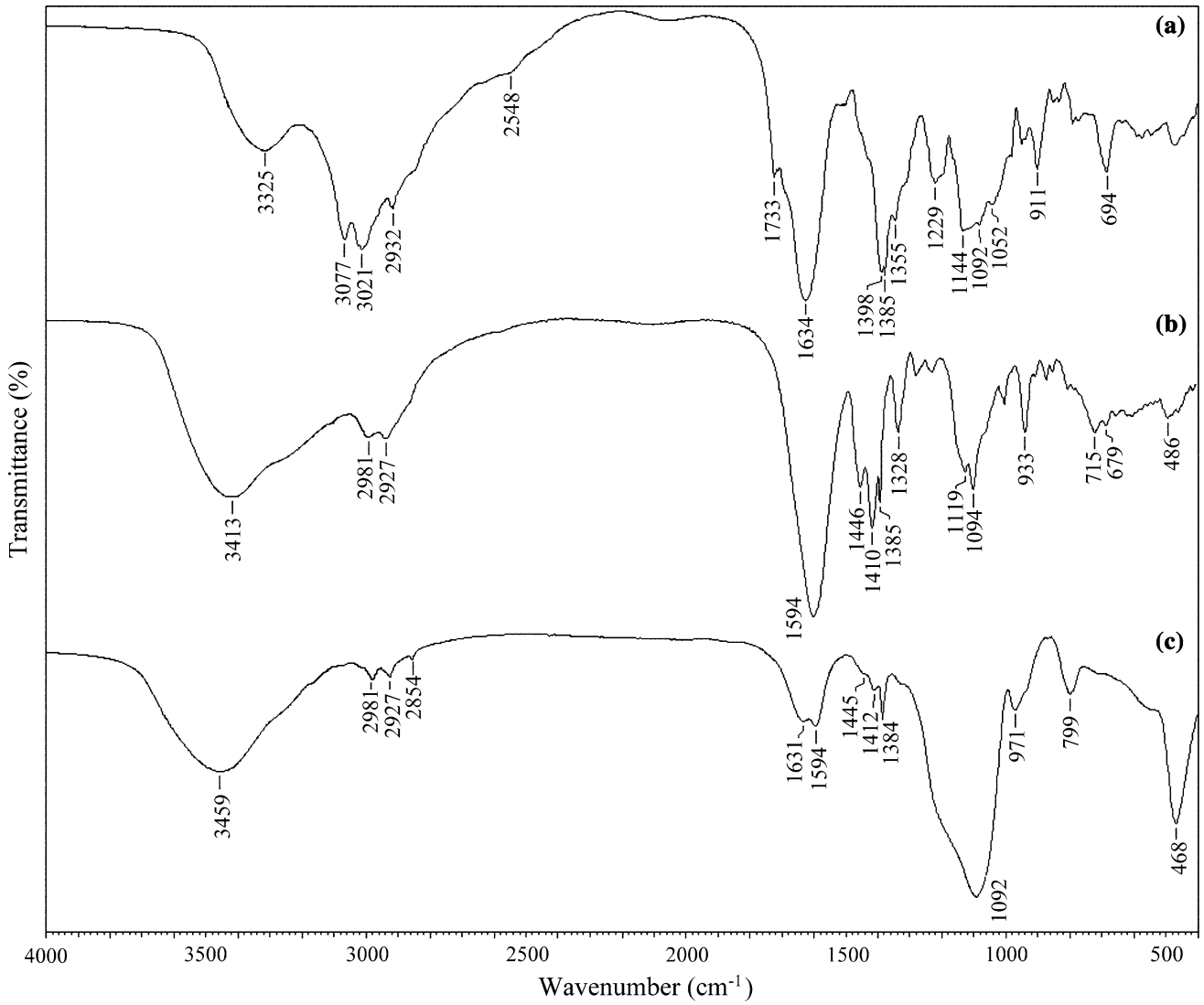

Fig. 2 FT-IR spectra of L2 (*a*) EuL2 (*b*) and EuL2/SiO_2 (*c*) in KBr pellets

stretching vibration frequencies of $-CH_2-$ groups are 2,855, 2,927, 2,981 cm^{-1}, and bending vibration frequencies are 1,385–1,446 cm^{-1}. The signal of ν_s (COO^-) appears at 1,410 cm^{-1}. The bands at 1,094–1,119 cm^{-1} are assigned to the stretching vibrations of Si–OH groups. Spectrum of EuL2 shows the absence of polycondensation of hydrolyzed fragments: there is no peak at 799 cm^{-1} corresponding to bending vibrations Si–O–Si. The bands at 679, 715 cm^{-1} correspond to vibrations C–Si.

Elemental analysis, mass spectrometry, ^1H NMR and FT-IR spectroscopy data suggest a similar structure for the complexes in series with the same ligand NdL1, EuL1, TbL1, YbL1, LuL1 and NdL2, EuL2, TbL2, YbL2, LuL2.

The presence of trialkoxysilyl fragment in the complexes provides their integration into siloxane matrix with the formation of covalently bonded hybrid materials. The reason for this is similar reactivity of trialkoxysilyl group of ligands or complexes and TEOS in the hydrolysis and copolycondensation processes that also leads to uniform distribution of the emitting centers in materials.

In FT-IR spectra of pure silica (SiO_2) signals corresponding to bending vibrations of O–Si–O and Si–O–Si are located at 468–799 cm^{-1}, respectively; bands of symmetric and asymmetric stretching vibrations of Si–O–Si appear at 970–1,088 cm^{-1}. In addition, some hydroxyl groups remaining in structure of silica give the band at 1,639 cm^{-1} (bending vibrations of Si–OH) and broad band at 3,459 cm^{-1} (stretching vibrations of O–H group). In spectra of hybrids the superposition of all mentioned above bands of inorganic carrier and the bands corresponding to lanthanide complexes (LnL1 or LnL2) is observed. In FT-IR spectra of obtained materials the position of LnL1 (LnL2) absorption bands almost does not change confirming the preservation of complex structure in resulting xerogels.

The scanning electronic microscopy (SEM) images of xerogel EuL2/SiO_2 (Fig. 3) indicate that material consists of particles with irregular form and size about 20 μm (Fig. 3a) and more shallow particles with sizes about 1 μm (Fig. 3b). It is known that the microstructure of sol–gel materials significantly depends of the synthesis conditions and the key role is played by the formation rate and the growth rate of the sol particles during the stage of sol formation [9]. Thus, at pH < 7 the rate of particles formation is greater than the rate of growth that resulting in a large number of little particles (less than 10 nm) which form a three-dimensional structure. At pH = 7–10 the growth rate of particles dominates and their size can reach about 500 nm. On the photo the formation of spherical nanoparticles could not be observed that suggests their aggregation with forming of a three-dimensional matrix on the early stages of growth (up to 3–5 nm).

Before discussing the luminescence spectra of obtained hybrid materials it's necessary to understand the role played by the hybrid aminopolycarboxylic-silica matrix in the sensitization of lanthanide luminescence. Under the excitation of hybrid matrices L1(L2)/SiO_2 in a wide spectral range (280–400 nm) two fluorescence bands are observed in the spectra: one at 330–350 nm which is excited at 260–300 nm, and the other at 400–475 nm excited at 320–400 nm. Similar emission spectra were observed for silica nanoparticles, which surface was modified with DTPA molecules [13]. This suggests at least two possible mechanisms responsible for the matrix luminescence. Its nature is not entirely established: according to some published data it is associated with defect centers in the silica [14] or the charge transfer process between silicon and oxygen [15], others claim that it is caused by carbon/oxygen impurities [16] and nitrogen-centered effects [17, 18].

The excitation and emission spectra of Eu(III)-containing xerogels are shown in Fig. 4.

The excitation spectra consist of symmetric and broad band ranging from 300 to 400 nm. The maximum of this band coincides with the excitation spectra of hybrid matrices (L1/SiO_2, L2/SiO_2) that confirms the efficient energy transfer to the Ln(III) ion. As can be seen from Fig. 4a the matrix is capable to transfer much more energy to the lanthanide ion than it absorbs at 394 nm (transition $^7F_0 \rightarrow {}^5L_6$). The corresponding emission spectrum contains $^5D_0 \rightarrow {}^7F_J$ (J = 0, 1, 2, 3, 4) transition lines of Eu(III) with the red emission transition $^5D_0 \rightarrow {}^7F_2$ as the most prominent group. The observed transitions are mainly of an electric dipole (ED) nature, except the $^5D_0 \rightarrow {}^7F_1$ line which has a predominant magnetic dipole (MD) contribution.

The 4f-luminescence intensity of obtained xerogels was evaluated by comparing with the corresponding molecular complexes (Eu-EDTA, Eu-DTPA). The luminescence intensity of EuL1/SiO_2 is about 63 % from Eu-EDTA intensity, and intensity of EuL2/SiO_2 is 72 % from Eu-DTPA. When assessing these values the concentration of the ion-emitter in the sample should also be taken into account. For example, the weight content of Eu(III) ion in EuL2/SiO_2 is 6.67 times lower in comparison with the Eu-DTPA. The 4f-luminescence intensity of EuL2/SiO_2 is 1.5 times higher than of EuL1/SiO_2. In the resulting xerogels compared to molecular complexes a slight increase of Eu(III) excited state lifetime is observed: from 329 μs in Eu-EDTA to 343 μs in EuL1/SiO_2 and from 625 μs in Eu-DTPA to 672 μs in EuL2/SiO_2 (Table 1).

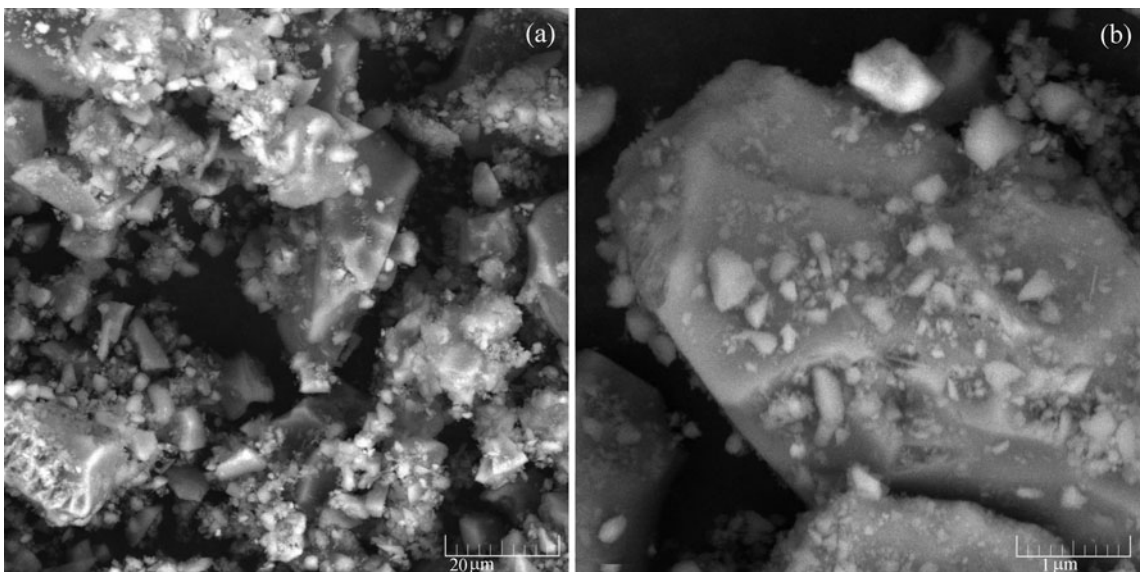

Fig. 3 SEM images of the sample EuL2/SiO_2

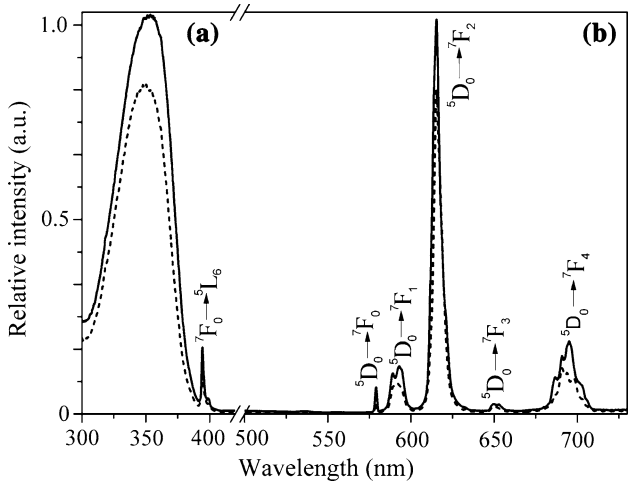

Fig. 4 Excitation (*a*) and emission (*b*) spectra of EuL1/SiO_2 (*dash line*) and EuL2/SiO_2 (*solid line*), 298 K, $\lambda_{ex} = 350$ nm, $\lambda_{em} = 615$ nm

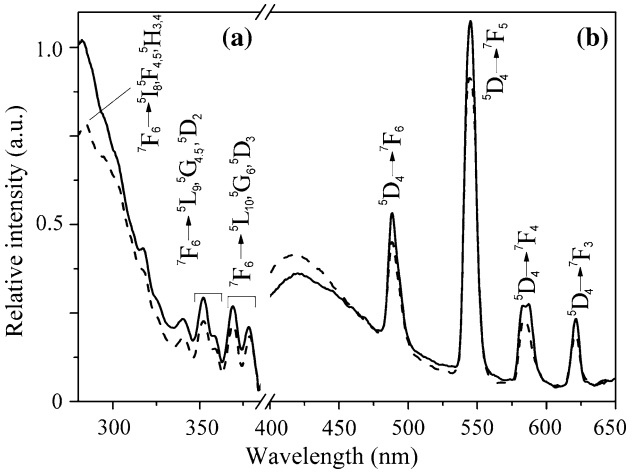

Fig. 5 Excitation (*a*) and emission (*b*) spectra of TbL1/SiO_2 (*dash line*) and TbL2/SiO_2 (*solid line*), 298 K, $\lambda_{ex} = 350$ nm, $\lambda_{em} = 545$ nm

In contrast to the Eu(III)-containing materials, in samples doped with Tb(III) complexes such significant energy transfer from the hybrid matrix was not observed (Fig. 5).

In the excitation spectrum of the 4f-luminescence (545 nm) only characteristic f–f transitions bands of the Tb(III) ion are presented. The luminescence spectrum of TbL1/SiO_2 and TbL2/SiO_2 registered under excitation 350 nm shows intense wide band of matrix fluorescence at 420 nm and bands corresponding to the Tb(III) transitions $^5D_4 \rightarrow {}^7F_J$ (J = 3, 4, 5, 6). The integrated intensity of the matrix fluorescence is two times larger than the 4f-luminescence, which intensity in the case of TbL1/SiO_2 is only 13.0 % of Tb-EDTA and 12.0 % in TbL2/SiO_2 in comparison with Tb-DTPA. The overall decrease in intensity is approximately proportional to decrease of Tb(III) weight content in all obtained samples.

Lifetime of Tb(III) excited state in the xerogels as well as in the case of Eu(III), slightly increases (Table 1). 4f-Luminescence decay curves for all hybrid materials can be fitted with monoexponential functions, which indicate the existence of only one type of emitting centers in the materials. Values of 4f-luminescence intensity and lifetime obtained from different points on the surface of the solid samples are within the experimental error (±5 %) indicating a homogeneous distribution of emitting centers in xerogels. So, excitation at 350 nm leads both to 4f-luminescence of Tb(III) and fluorescence of hybrid matrix, which excitation energy is not transferred to the lanthanide ion. The reason for this is probably in the location of energy levels of the matrix and Tb(III) ion.

Table 1 Spectral-luminescent properties of hybrid materials

Sample	λ_{max}, nm	$I_{4f\text{-}lum}$, %	τ, μs
Eu-EDTA	578, 592, 615, 694	82.3	329
Eu-DTPA	579, 592, 615, 693	100.0	625
EuL1/SiO_2	579, 592, 615, 691	52.5	343
EuL2/SiO_2	579, 593, 615, 695	72.3	672
Tb-EDTA	488, 544, 583, 621	84.1	1,162
Tb-DTPA	487, 544, 581, 620	100.0	1,930
TbL1/SiO_2	488, 545, 583, 621	10.9	1,213
TbL2/SiO_2	488, 545, 583, 621	12.0	1,973

Mass content of Ln(III) in Ln-EDTA was about 34.3–35.6 %, in Ln-DTPA—about 28.0–29.0 %, in LnL1/SiO_2—4.3–4.5 % and in LnL2/SiO_2—4.1–4.3 %

It is known that the difference between the emitting state of the donor and the resonance state of Ln(III) must be in some optimal range for the possibility of effective energy transfer. According to the literature data this energy gap is approximately 1,500–2,500 cm^{-1} [1, 2]. The energy of the singlet states of LuL1/SiO_2 and LuL2/SiO_2 amounts to 23,750–24,210 cm^{-1}, respectively, and the energy of the triplet states—22,420–21,900 cm^{-1}, respectively. Such arrangement of excited states is acceptable for efficient energy transfer to Eu(III) ion, which resonance state $^5D_0$ is located at 17,280 cm^{-1}. The resonance states of Yb(III) and Nd(III) are about 10,200–11,460 cm^{-1}, respectively. Despite the large energy gap transfer for such objects is possible. Efficient luminescence sensitization of Tb(III), which resonance level $^5D_4$ is located at 20,500 cm^{-1}, is not observed, probably due to the high probability of reverse energy transfer from the metal to the modified matrix (Fig. 6).

As well as Tb(III)-containing, hybrids doped with Yb(III) and Nd(III) aminopolycaboxylates demonstrate both matrix fluorescence and 4f-luminescence in the near-infrared region. In the excitation spectra of YbL1/SiO_2 and YbL2/SiO_2 only matrix absorption band with a maximum

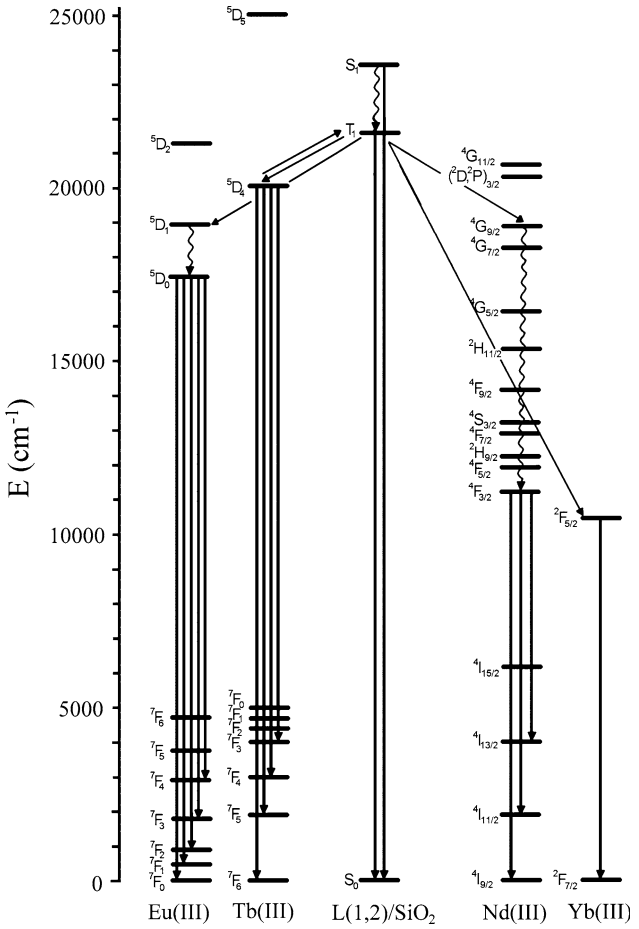

Fig. 6 Energy level diagram of the Ln(III)-containing hybrid materials

at 350 nm is observed (absorption band of Yb(III) is located at 980 nm). The luminescence spectra contain intense band of matrix fluorescence, which is quenched by 60–80 % in comparison with $LuL1/SiO_2$ and $LuL2/SiO_2$. The single transition of Yb(III) $^2F_{5/2} \rightarrow {}^2F_{7/2}$ appears in the form of band at 980 nm.

In the luminescence spectra of $NdL1/SiO_2$ and $NdL2/SiO_2$ under excitation at 350 nm besides intense matrix fluorescence three 4f-luminescence bands at 893, 1,065–1,330 nm corresponding to $^4F_{3/2} \rightarrow {}^4I_J$ (J = 9/2, 11/2, 13/2) transitions of Nd(III) are observed. In general, 4f-luminescence intensity of these materials about 2.5 times lower than for Yb(III)-containing samples. It should be noted that for all lanthanide ions 4f-luminescence intensity increases from $LnL1/SiO_2$ to $LnL2/SiO_2$. This fact can be explained by the larger number of water molecules coordinated to Ln(III) in the case of $LnL1/SiO_2$, which are able to quench 4f-luminescence.

The stability of lanthanide-containing hybrid materials towards water was evaluated as follows. Powdered silica samples (1 g) were mixed with 50 ml of water at 25 °C. After staying for one day or 1 week they were dried under the same conditions as described in the synthesis. It was found for Eu(III)- and Tb(III)-containing samples that the luminescence intensity decreased by 2–3 and 4–5 % in comparison with the starting materials after contact with water for a day and for a week, respectively.

Photostability of obtained samples was investigated by UV-irradiation of the samples with a 250 W high-power Hg arc lamp (DRSh-250, PhysPribor, Russia) for 6 h. As a result, it was found that the 4f-luminescence intensity is reduced as follows: $EuL1/SiO_2$—86 %, $YbL1/SiO_2$—83 %, $NdL1/SiO_2$—81 %, $TbL1/SiO_2$—79 %, $EuL2/SiO_2$—87 %, $YbL2/SiO_2$—84 %, $NdL2/SiO_2$—84 %, $TbL2/SiO_2$—81 % (the initial luminescence intensity of the corresponding complexes was taken as 100 %).

In most of the publications, devoted to lanthanide-doped hybrid materials, complexes with organic ligands, which act as photosensitizers of 4f-luminescence, are considered [3–8]. Much less publications are devoted to study of the energy transfer from the hybrid matrix to Ln(III). According to some reported data [19–21], the efficiency of such transfer is rather low. It should be noted that in our case the main factors leading to the possibility of efficient energy transfer to Eu(III) ion were optimal energy gap, presence of the strongly chelating ligands and the synthesis conditions (relatively high temperature and low pressure in the last stage of drying), which causes the maximal possible removal of water molecules from materials and approaching of matrix emitting centers with complex molecules as a result of matrix compression during drying stage.

4 Conclusions

Hybrid organic–inorganic materials, where Ln(III) aminopolycarboxylates were immobilized in the structure of silica matrix by covalent bonds, were obtained. It is shown that the sensitization efficiency of 4f-luminescence strongly depends on the position of the excited energy levels of Ln(III). Silica matrix modified with aminopolycarboxylic fragments is able to transfer efficiently the excitation energy to Eu(III) ion. While the content of an ion-emitter in hybrids decreases in 6–7 times the 4f-luminescence intensity persists on the level of 63–72 % compared with the molecular complexes. For all lanthanide ions some increase in the lifetime of the excited states was recorded, which is a consequence of the reduction of non-radiative energy losses. Based on complexonates of Tb(III), Yb(III) and Nd(III) we obtained materials emitting in a wide spectral range due to superposition of matrix fluorescence and 4f-luminescence.

Acknowledgments This work was supported by the National Academy of Sciences of Ukraine (DCNTP "Nanotechnology and

nanomaterials", Project 6.22.7.43 and Grant of NAS of Ukraine for young scientists in 2011–2012 years).

References

1. Bünzli JC, Piguet C (2005) Taking advantage of luminescent lanthanide ions. Chem Soc Rev 34:1048–1077
2. Hanninen P, Harma H (2011) Lanthanide luminescence: photophysical, analytical and biological aspects. Springer-Verlag, Berlin
3. Binnemans K (2009) Lanthanide-based luminescent hybrid materials. Chem Rev 109:4283–4374
4. Yan B (2012) Recent progress in photofunctional lanthanide hybrid materials. RSC Adv 2:9304–9324
5. Escribano P, Julian-Lopez B, Planelles-Arago J, Cordoncillo E, Viana B, Sanchez C (2008) Photonic and nanobiophotonic properties of luminescent lanthanide-doped hybrid organic-inorganic materials. J Mater Chem 18:23–40
6. Carlos LD, Ferreira RA, Bermudez VZ, Julian-Lopez B, Escribano P (2011) Progress on lanthanide-based organic-inorganic hybrid phosphors. Chem Soc Rev 40:536–549
7. Armelao L, Quici S, Barigelletti F, Accorsi G, Bottaro G, Cavazzini M, Tondello E (2010) Design of luminescent lanthanide complexes: from molecules to highly efficient photo-emitting materials. Coord Chem Rev 254:487–505
8. Carlos LD, Ferreira RAS, Bermudez VZ (2009) Lanthanide-containing light-emitting organic-inorganic hybrids: a bet on the future. Adv Mater 21:509–534
9. Brinker CJ, Scherer GW (1990) Sol–gel science: the physics and chemistry of sol–gel processing. Academic Press, New York
10. Choppin GR, Baisden PA, Khan SA (1979) Nuclear magnetic resonance studies of diamagnetic metal-diethylenetriaminepentaacetate complexes. Inorg Chem 18:1330–1332
11. Baisden PA, Choppin GR, Garrett BB (1977) Nuclear magnetic resonance studies of diamagnetic metal-aminopolycarboxylate complexes. Inorg Chem 16:1367–1372
12. Yan B, Zhang H, Wang S, Ni J (1997) Luminescence properties of the ternary rare earth complexes with β-diketones and 1,10-phenanthroline incorporated in silica matrix by a sol–gel method. Mater Chem Phys 51:92–96
13. Pinho SLC, Faneca H, Geraldes CFG, Delville MH, Carlos LD, Rocha J (2012) Lanthanide-DTPA grafted silica nanoparticles as bimodal-imaging contrast agents. Biomaterials 33:925–935
14. Yoldas BE (1990) Photoluminescence in chemically polymerized SiO_2 and Al_2O_3-SiO_2 systems. J Mater Res 5:1157–1158
15. Garcia J, Mondragon M, Tellez C (1995) Blue emission in tetraethoxysilane and silica gels. Mater Chem Phys 41:15–17
16. Green WH, Le KP, Grey J, Au TT, Sailor MJ (1997) White phosphors from a silicate-carboxylate sol–gel precursor that lack metal activator ions. Science 276:1826–1828
17. Brankova T, Bekiari V, Lianos P (2003) Photoluminescence from sol–gel organic/inorganic hybrid gels obtained through carboxylic acid solvolysis. Chem Mater 15:1855–1859
18. Carlos LD, Ferreira RAS, Pereira RN, Assuncao M, Bermudez VZ (2004) White-light emission of amine-functionalized organic/inorganic hybrids: emitting centers and recombination mechanisms. J Phys Chem B 108:14924–14932
19. Bermudez VZ, Carlos LD, Duarte MC, Silva MM, Silvac CJR, Smith MJ, Assuncao M, Alcacer L (1998) A novel class of luminescent polymers obtained by the sol–gel approach. J Alloys Compd 275–277:21–26
20. Tiseanu C, Parvulescu VI, Kumke MU, Dobrolu S, Gessner A, Simon S (2009) Effects of support and ligand on the photoluminescence properties of siliceous grafted europium complexes. J Phys Chem C 113:5784–5791
21. Lipowska B, Klonkowski AM (2008) Energy transfer and surface plasmon resonance in luminescent materials based on Tb(III) and Ag or Au nanoparticles in silica xerogel. J Non-Cryst Solids 354:4383–4387